



Contents lists available at ScienceDirect

Biochemical and Biophysical Research Communications

journal homepage: [www.elsevier.com/locate/ybbrc](http://www.elsevier.com/locate/ybbrc)



# Oxaliplatin triggers *necrosis* as well as apoptosis in gastric cancer SGC-7901 cells



Ping Wu <sup>a</sup>, Xueping Zhu <sup>a</sup>, Wei Jin <sup>b</sup>, Shumei Hao <sup>a</sup>, Qi Liu <sup>a</sup>, Linjie Zhang <sup>a,\*</sup>

<sup>a</sup> Department of Immunology, Anhui Medical University, Hefei 230032, China

<sup>b</sup> Department of Otolaryngology, Chaohu Hospital of Anhui Medical University, Chaohu 238000, China

## ARTICLE INFO

### Article history:

Received 13 February 2015

Available online 9 March 2015

### Keywords:

Apoptosis

Necrosis

Necrostatin-1

RIP1

AIF

PARP-1

## ABSTRACT

Intrinsic apoptotic pathway is considered to be responsible for cell death induced by platinum anticancer drugs. While in this study, we found that, *necrosis* is an indispensable pathway besides apoptosis in oxaliplatin-treated gastric cancer SGC-7901 cells. Upon exposure to oxaliplatin, both apoptotic and necrotic features were observed. The majority of dead cells were double positive for Annexin V and propidium iodide (PI). Moreover, mitochondrial membrane potential collapsed and caspase cascades were activated. However, ultrastructural changes under transmission electron microscope, coupled with the release of cellular contents, demonstrated the rupture of the plasma membrane. Oxaliplatin administration did not stimulate reactive oxygen species (ROS) production and autophagy, but elevated the protein level of Bmf. In addition, receptor interacting protein 1 (RIP1), but not receptor interacting protein 3 (RIP3) and its downstream components participated in this death process. Necrostatin-1 (Nec-1) blocked oxaliplatin-induced cell death nearly completely, whereas z-VAD-fmk could partially suppress cell death. Oxaliplatin treatment resulted in poly(ADP-ribose) polymerase-1 (PARP-1) overactivation, as indicated by the increase of poly(ADP-ribose) (PAR), which led to NAD<sup>+</sup> and ATP depletion. PARP-1 inhibitor, olaparib, could significantly block oxaliplatin-induced cell death, thus confirming that PARP-1 activation is mainly responsible for the cytotoxicity of oxaliplatin. Phosphorylation of H2AX at Ser139 and translocation of apoptosis-inducing factor (AIF) are critical for this death process. Taken together, these results indicate that oxaliplatin can bypass canonical cell death pathways to kill gastric cancer cells, which may be of therapeutic advantage in the treatment of gastric cancer.

© 2015 Published by Elsevier Inc.

## 1. Introduction

Programmed cell death (PCD) is a ubiquitous process to sustain tissue homeostasis and health, and evading PCD is one of the hallmarks of cancer. Conversely, inducing cell death by pharmacological means is the basis of cancer therapy. Unquestionably, apoptosis is the best-characterized form of PCD. However, over the past decade, extensive studies have uncovered a growing number of non-apoptotic cell death pathways, such as lysosomal-mediated cell death, autophagic cell death and necroptosis.

Necrosis, which was thought to be a passive event as a result of overwhelming insults, may be executed through a regulated mechanism termed necroptosis or programmed necrosis. Several stimuli can trigger the necrotic response, such as cytokines, pathogen, alkylating DNA damage, excitotoxins or irradiation [1].

Nowadays the most extensively studied models are tumor necrosis factor- $\alpha$  (TNF- $\alpha$ )-induced receptor interacting protein 1 (RIP1)/receptor interacting protein 3 (RIP3)-dependent pathway and *N*-methyl-*N'*-nitro-*N*-nitrosoguanidine (MNNG)-induced poly(ADP-ribose) polymerase-1 (PARP-1) pathway.

Stimulation with TNF- $\alpha$  leads to the activation of RIP1, then RIP3 is recruited to RIP1, the two kinases phosphorylate each other [2]. Necrostatin-1 (Nec-1), a small-molecule inhibitor of necroptosis, is a selective inhibitor of RIP1 kinase [3]. RIP3 in turn phosphorylates mixed lineage kinase domain-like protein (MLKL) [4]. RIP1, RIP3 and MLKL are the core components of the necrosome. Downstream of the necrosome are phosphoglycerate mutase family member 5 (PGAM5), which specifically associates with the necrosome, resulting in PGAM5 phosphorylation and activation. PGAM5 recruits the mitochondrial fission factor dynamin-related protein 1 (Drp1) and activates its GTPase activity by dephosphorylating Drp1. Drp1 activation caused mitochondrial fragmentation and eventually, necroptosis [5].

\* Corresponding author.

E-mail address: [zlj33@ahmu.edu.cn](mailto:zlj33@ahmu.edu.cn) (L. Zhang).

In response to DNA-alkylating agents such as MNNG, DNA repair enzyme PARP-1 was overactivated, resulting in the massive synthesis of poly(ADP-ribose) (PAR) from  $\text{NAD}^+$  and, in consequence, to the rapid depletion of intracellular  $\text{NAD}^+$  and ATP pools [6] and calpains activation [7]. Calpains cleave Bid into tBid, which redistributes from the cytosol to mitochondria, where it facilitates Bax activation. Furthermore, Bax provokes mitochondrial damage and favors the release of apoptosis-inducing factor (AIF) from mitochondria to the cytosol and nucleus [8]. Upon transferring to the nucleus, AIF associates with cyclophilin A (CypA) and H2AX to generate a DNA-degrading complex that promotes chromatinolysis and cell-viability loss [9].

Oxaliplatin is the third generation of platinum anticancer drugs that is widely used in various cancers. As an alkylating agent, oxaliplatin works by binding to DNA leading to oxaliplatin-DNA adducts. The mechanism whereby DNA adducts kill cells is not fully understood. Is oxaliplatin-induced cell death always produced by apoptosis? Whether oxaliplatin could induce necrosis in gastric cancer cells needs to be examined. We report here that although oxaliplatin activates caspase cascade, it kills SGC-7901 cells predominantly by necrosis dependent on RIP1. And PARP-1 over-activation-induced energy depletion, H2AX phosphorylation and AIF translocation are critical in this process.

## 2. Materials and methods

### 2.1. Cell culture

Human gastric cancer cell SGC-7901 was obtained from Type Culture Collection of Chinese Academy of Sciences. They were cultured in RPMI 1640 medium (Gibco) containing 10% fetal bovine serum (Hyclone).

### 2.2. Reagents

Oxaliplatin was purchased from Jiangsu Hengrui Medicine. PAR antibody and Nec-1 were provided by Enzo Life Sciences. Necrosulfonamide (NSA) and z-VAD-fmk were obtained from Calbiochem. Mdivi-1 was from Sigma–Aldrich. Olaparib was purchased from Selleck. Antibodies against caspase-3, PARP-1, Bcl-2, Mcl-1 and AIF were from Santa Cruz Biotechnology. Antibodies against Bcl-X<sub>L</sub>, XIAP, cIAP1, cIAP2, HMGB1, caspase-9, cyclophilin A, LC3,  $\gamma$ H2AX were obtained from Cell Signaling Technology. Bmf and COXIV antibodies were from Proteintech.

### 2.3. Cell viability assay (MTS)

Cell viability assay was performed using the CellTiter 96 AQueous One Solution Assay Kit (Promega) following manufacturer's instruction. Briefly, cells were seeded in 96-well plates and allowed to grow for 24 h followed by the desired treatment. 20  $\mu$ l reagent was added to the cell culture medium, and incubated at 37 °C for 1 h, optical density at 490 nm was readed on a microplate reader (BioTek).

### 2.4. Flow cytometry

Cells were seeded in 24-well plates and allowed to reach exponential growth before treatment. Adherent and floating cells were collected. To measure apoptotic and necrotic cell death, cells were incubated with 5  $\mu$ l Annexin V-FITC and 5  $\mu$ l propidium iodide (PI) (BD Pharmingen) for 15 min in the dark. To measure mitochondrial membrane potential ( $\Delta\Psi$ m), cells were stained with 10  $\mu$ g/ml of JC-1 (Fanbo Biochemicals) at 37 °C for 15 min. For detection of reactive oxygen species (ROS), cells were

incubated with 10  $\mu$ M 2',7'-Dichlorofluorescein diacetate (DCF-DA) (Sigma–Aldrich) at 37 °C for 20 min. After washing with PBS, cells were analyzed using a FACSVerse flow cytometer (BD).

### 2.5. Transmission electron microscopy

Cells were harvested, fixed in 2.5% glutaraldehyde, rinsed with PBS and post-fixed in 1% osmium tetroxide, dehydrated through a series of graded ethanol. Samples were placed in propylene oxide, incubated in propylene oxide/epoxy resin mixture and embedded in pure resin. After polymerized in 60 °C oven, 70 nm sections were cut, and stained with 2% uranyl acetate and lead citrate. Images were captured using a JEM-1230 transmission electron microscope (JEOL).

### 2.6. Lactate dehydrogenase (LDH) release

The LDH-cytotoxicity assay kit (Beyotime) quantitates the activity of LDH released from damaged cells. After treatment, the plate was centrifuged at 400 g for 5 min. 120  $\mu$ l supernatant was transferred into a clear 96-well plate, and 60  $\mu$ l reaction mixture was added to each well. The plate was incubated in the dark for 30 min, the absorbance at 490 nm was measured. The activity of LDH was calculated according to the standard curve.

### 2.7. Measurement of intracellular $\text{NAD}^+$ and ATP levels

Intracellular  $\text{NAD}^+$  was determined by the EnzyChrom  $\text{NAD}^+$ /NADH assay kit (BioAssay Systems). Cell pellets were homogenized with 100  $\mu$ l NAD extraction buffer, then heated at 60 °C for 5 min. Then 20  $\mu$ l assay buffer and 100  $\mu$ l NADH extraction buffer were added to neutralize the extracts. After centrifuge, 40  $\mu$ l supernatant of each sample was mixed with 80  $\mu$ l working reagent. Optical density for time “zero” ( $\text{OD}_0$ ) at 570 nm and  $\text{OD}_{15}$  after 15-min incubation were recorded. First compute the  $\Delta\text{OD}$  for each standard and sample by subtracting  $\text{OD}_0$  from  $\text{OD}_{15}$ . Plot the standard  $\Delta\text{OD}$ 's and the  $\text{NAD}^+$  concentration of the sample was computed. The ATP level was measured by the luciferin/luciferase method using an ATP determination kit (Beyotime). The cell lysates were centrifuged, 10  $\mu$ l supernatant was mixed with 100  $\mu$ l ATP detection solution. Relative light unit (RLU) was immediately measured using GloMax-Multi Jr Luminometer (Promega). The concentration of ATP was calculated according to the standard curve.

### 2.8. Immunofluorescence

Cells were fixed in 2% paraformaldehyde and permeabilized in 0.1% Triton X-100, followed by incubation with anti- $\gamma$ H2AX antibody and Alexa Fluor 488-conjugated goat anti-rabbit IgG (ZSbio). Fluorescences were observed in a Nikon Eclipse 80i microscope. To visualize nuclei, cells were co-stained with Hoechst 33342.

### 2.9. Western blotting

The mitochondrial and cytosolic fractions were prepared using a Mitochondria isolation kit (Beyotime) according to the manufacturer's instruction. For detection of cyclophilin A and HMGB1 release, supernatants were concentrated using Amicon ultra centrifugal filters (Millipore). For whole cell lysates, cells were lysed in RIPA buffer before centrifugation. Protein concentrations were determined by the BCA assay (Beyotime). A total of 20  $\mu$ g of protein was electrophoresed on SDS-PAGE gels and transferred to nitrocellulose membranes (Amersham Biosciences). Membranes were blocked, incubated with primary antibodies, and subsequently with HRP-conjugated secondary antibodies. Labeled bands were detected

by SuperSignal West Femto Chemiluminescent Substrate (Pierce), and images were captured in a Gel Imaging System 4500 (Tanon).

### 2.10. siRNA transfection

Three individual siRNA oligos target human RIP1 (001–003) or RIP3 (004–006) and negative control were synthesized by RiboBio. Cells were transfected with 100 nM siRNA in Opti-MEM (Invitrogen) using Lipofectamine 2000 reagent (Invitrogen) according to the manufacturer's instructions. Efficiency of siRNA was measured by Western blotting 72 h after transfection.

### 2.11. Statistical analysis

Data are expressed as means  $\pm$  SD. The statistical significance of intergroup differences was determined using Student's *t*-test.

## 3. Results

### 3.1. Oxaliplatin induces cell death in gastric cancer SGC-7901 cells

To identify the type of cell death induced by oxaliplatin, we first examined the biochemical events in SGC-7901 cells. Dual staining with Annexin V-FITC and PI was used to discriminate apoptosis and necrosis. As depicted in Fig. 1A, the majority of dead cells became positive for both Annexin V and PI, and some only for PI, even at 24 h when only a small proportion of cells died. Furthermore, cell death was associated with reduction in  $\Delta\Psi_m$  (Fig. 1B), indicating that mitochondrial depolarization is involved in this process. Activation of caspase-9 and caspase-3, together with PARP-1 cleavage (Fig. 1C) were also observed, suggesting the activation of the mitochondrial apoptotic pathway. Oxaliplatin treatment did not cause obvious alterations in Bcl-2 family proteins and inhibitor of apoptosis proteins (IAPs) family members except slight decrease of XIAP (Fig. 1D).

### 3.2. Oxaliplatin triggers plasma membrane rupture in SGC-7901 cells

LDH is a stable cytoplasmic enzyme present in all cells and rapidly released into the cell culture supernatant upon damage of the plasma membrane. After exposure to oxaliplatin for 36 h, the activity of LDH in the culture medium increased greatly (Fig. 2A). Biomarkers of necrosis being well documented are the release of high mobility group box-1 protein (HMGB1) and cyclophilin A (CypA). CypA was observed in the supernatant of oxaliplatin-treated cells at 36 h, subsequently HMGB1 at 48 h (Fig. 2B), suggesting that the integrity of the plasma membrane is compromised. Transmission electron microscopic analysis is the gold standard for judging necrosis. Rupture of the plasma membrane and loss of cytoplasmic contents were readily detected after exposure to oxaliplatin for 32 h. Besides, nuclear margination and condensation were also observed (Fig. 2C). Thus, the above results show that oxaliplatin primarily induces necrosis in SGC-7901 cells. ROS and autophagy are proposed to be executioners of necroptosis. But there were no ROS production (Fig. 2D) and conversion of LC3-I to LC3-II (Fig. 2E), implicating that oxidative stress and autophagy were not associated with oxaliplatin-induced cell death. While the protein level of Bmf, a protein that is tightly linked with necroptosis, was elevated with time (Fig. 2E).

### 3.3. RIP1, but not RIP3 and its downstream components, are involved in this death process

As RIP1 has an important role in initiating necroptosis, we examined whether it is involved in necrosis of SGC-7901 cells. As

shown in Fig. 3A, Nec-1 significantly suppressed oxaliplatin-mediated cell death, almost all of the cells were rescued. Notably, pan-caspase inhibitor (z-VAD-fmk) could also attenuate cell death but to a lesser extent. Moreover, Nec-1 efficiently inhibited the release of LDH (Fig. 3B), CypA and HMGB1 (Fig. 3C). Knockdown of RIP1 by siRNA could decrease cell death to varying degrees, but the inhibitory effect was limited (Fig. 3D and F). Knockdown of RIP3 by siRNA (Fig. 3E and F) could not prevent SGC-7901 cells from dying. Moreover, MLKL inhibitor (NSA) or Drp1 inhibitor (Mdivi-1) had little effect on oxaliplatin-induced cell death (Fig. 3A), suggesting that RIP3 and its downstream molecules are not involved in this process.

### 3.4. H2AX phosphorylation and AIF relocation are associated with oxaliplatin-induced necrosis

DNA-alkylating agents have been shown to activate the enzymatic activity of PARP-1, and hyperactivation of PARP-1 results in a rapid depletion of cellular energy. Upon oxaliplatin treatment, PARP-1 was activated, as indicated by the increase of PAR polymers (Fig. 4A), and decreases in  $\text{NAD}^+$  and ATP levels occurred with time (Fig. 4B). In addition, olaparib, a potent inhibitor of PARP-1, could effectively impair the activation of PARP-1 and formation of PAR (Fig. 4A), and attenuated oxaliplatin-induced necrosis (Fig. 3A). In PARP-1-mediated cell death, AIF is translocated from mitochondria to the cytosol and eventually nucleus, where it associates with Ser139-phosphorylated H2AX ( $\gamma\text{H2AX}$ ) to create a DNA-degrading complex. Immunofluorescence successfully revealed a time-dependent H2AX phosphorylation, the intensity of fluorescence reached a peak at 36 h, then declined thereafter (Fig. 4C). AIF redistribution from mitochondria to the cytosol was also observed after exposure to oxaliplatin for 24 h (Fig. 4D).

## 4. Discussion

During the past decade, cell death researchers have witnessed a gradual conceptual revolution: necrosis, which had been considered as a purely accidental cell death mode, can also be induced by finely regulated signaling pathways. The term necroptosis was firstly introduced by Degterev and his colleagues [10] in 2005 to describe that in the absence of caspases, ligation of TNF- $\alpha$  with its receptor would prime cells to necrotic cell death. At present, it has been established that necrotic cell death can be triggered by extrinsic signals such as death ligands and by intrinsic signals such as DNA damage.

Like cisplatin and carboplatin, oxaliplatin forms both inter- and intra-strand cross-links in DNA once it gets into a cell. It has been thought predominately to activate the mitochondrial apoptotic pathway. However, increasing evidences have demonstrated that platinum drugs, just as other DNA-damaging agents, may kill cells via another way, that is, necrosis [11].

The above results indicate that oxaliplatin-induced cell death exhibits both apoptotic and necrotic features. Activation of caspase-9 and caspase-3, appearance of 89 kDa band of PARP-1, together with z-VAD-fmk partial protection against cell death, suggested the induction of apoptosis. After treatment for 24 h, the full-length of PARP-1 disappeared, this is likewise due to autopoly (ADP-ribosyl) action of PARP-1 itself. The disappearance of the PARP-1 signal (full-length 116 kDa) is an indicator of PARP-1 activation rather than PARP-1 destruction. Moreover, oxaliplatin exposure resulted in collapse of  $\Delta\Psi_m$ , suggesting the involvement of mitochondria. Among those regulatory proteins in Bcl-2 family and IAP family members, most of them were not altered after treatment, except slight decrease of XIAP, this may be required for this death process.

In spite of activation of caspase cascade, oxaliplatin also resulted in permeability of the plasma membrane. This was directly

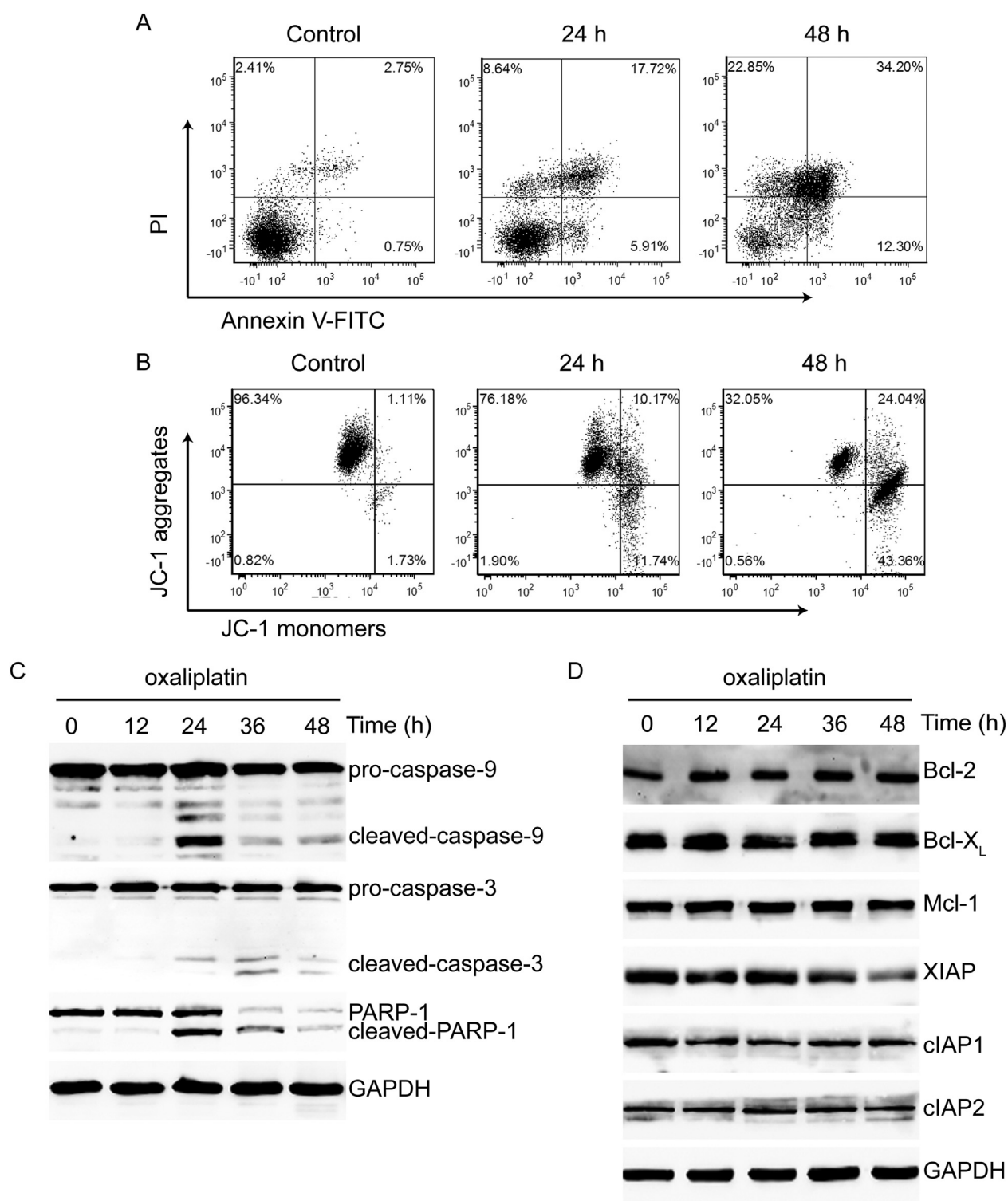


**Fig. 1.** Oxaliplatin induces cell death in gastric cancer SGC-7901 cells. (A, B) After the indicated time post oxaliplatin (50  $\mu$ g/ml) treatment, cells were labeled with Annexin V-FITC and PI to assess phosphatidylserine exposure and cell permeability, or JC-1 to detect  $\Delta\Psi_m$  by flow cytometry. Identical concentration of oxaliplatin was used in later experiments. (C, D) The protein level of caspase-9, caspase-3, PARP-1, Bcl-2, Bcl-X<sub>L</sub>, Mcl-1, XIAP, cIAP1 and cIAP2 before and after treatment with oxaliplatin were measured by Western blotting. GAPDH was used as the loading control.

evidenced by visualization of rupture of the plasma membrane and loss of cytoplasmic contents using transmission electron microscope. There were no obvious changes under light microscope until 24 h, when only about 30% of cells died. Among these dead cells, most of them showed PI-positive. Similarly, PI-positive-cells

accounted for four-fifths of dead cells at 48 h. It seems that the integrity of the plasma membrane was damaged as soon as the cell died. Nowadays double positive labeling was viewed as necrotic cells. It was reported that necrotic cells show Annexin V-positive/PI-negative staining before they become PI-positive. Nec-1 can



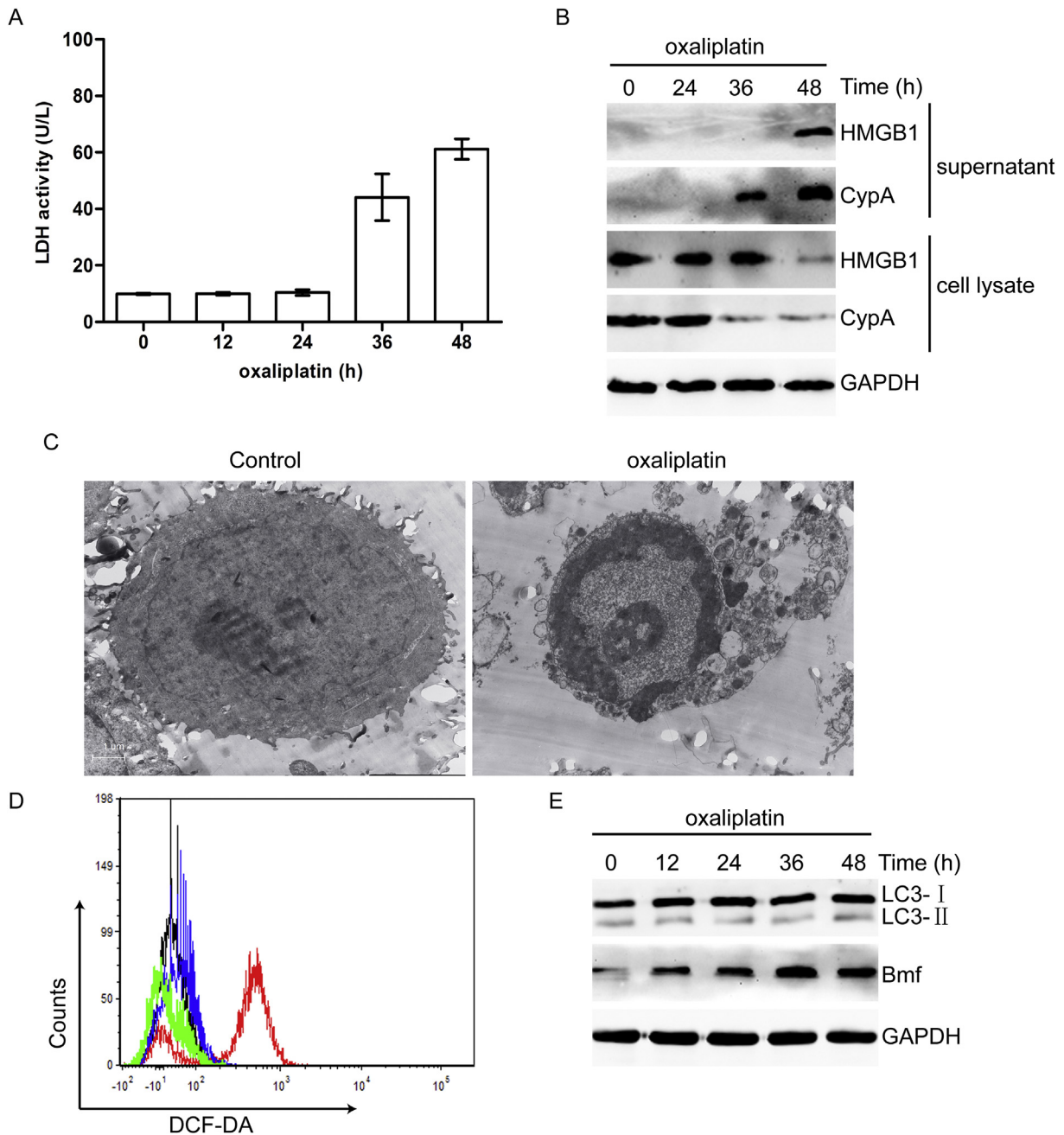


**Fig. 2.** Oxaliplatin compromises the integrity of the plasma membrane. (A) The activity of extracellular LDH was measured after exposure to oxaliplatin for different time points. (B) After treatment with oxaliplatin, the supernatant and cell lysate were analyzed by Western blotting using CypA and HMGB1 antibodies. (C) Transmission electron microscopy of the cells untreated (Control) or treated with oxaliplatin for 32 h. Representative images are shown. Bar: 1  $\mu$ m. (D) Cells treated with oxaliplatin were stained with DCF-DA to measure the level of ROS by flow cytometry. Black: Control. Blue: oxaliplatin (24 h). Green: oxaliplatin (48 h). Red: positive control, H<sub>2</sub>O<sub>2</sub> (20 min). (E) Western blotting of LC3-I/II and Bmf in cells before and after incubation with oxaliplatin. (For interpretation of the references to color in this figure legend, the reader is referred to the web version of this article.)

inhibit Annexin V-positive/PI-negative (as well as PI-positive) staining in necrotic but not in apoptotic cells [12]. Another clue came from the exposure of damage associated molecular patterns (DAMPs). CypA was released early in z-VAD-fmk-treated L929 cells [13]. By the same token, in oxaliplatin-treated SGC-7901 cells, the release of CypA was earlier than that of HMGB1. These molecules released into the extracellular space may drive a local inflammatory reaction *in vivo*.

ROS, autophagy and mitochondria are proposed to be downstream components of necroptosis. MEFs produced ROS in response to TNF stimulation [14], oxaliplatin induced high level of

ROS in HepG2 cells [15]. Autophagic vesicles are commonly observed in necroptotic cells, and treatment with autophagy inhibitor 3-MA are able to partially inhibit cell death [10]. However, in oxaliplatin-treated SGC-7901 cells, these views could not hold up. Evidences suggest that autophagy is capable of either promoting, suppressing, or not associated with necroptosis. Whether or not autophagy and ROS are involved is dependent on stimulus and cell type, it is unlikely to be a general mechanism. While a BH3-only protein, Bmf, identified in a siRNA screen for the genes involved in necroptosis [16], seems to be crucial to oxaliplatin-induced cell death.

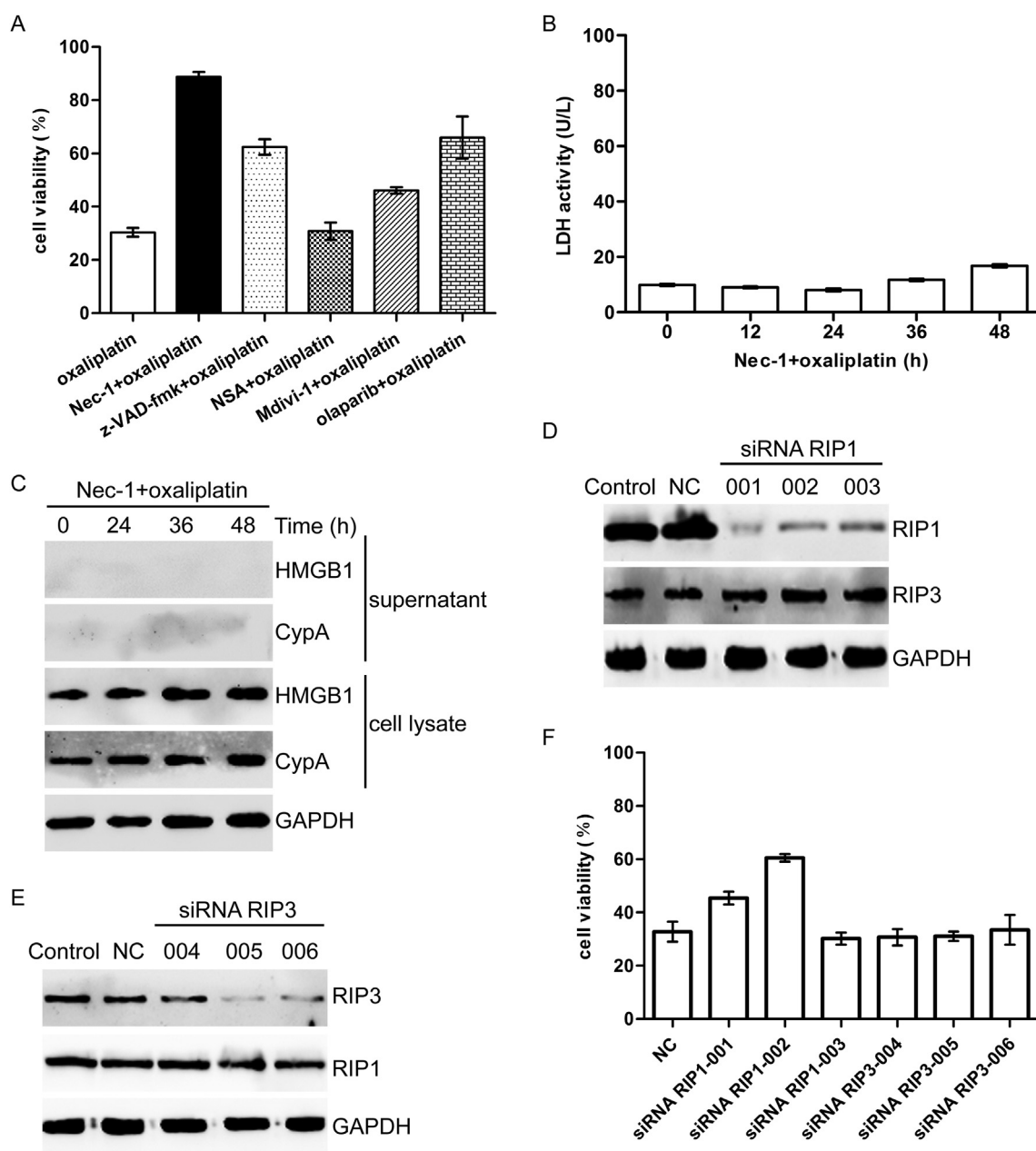


**Fig. 3.** Oxaliplatin-induced cell death is dependent on RIP1 but not RIP3. (A) Prior to oxaliplatin treatment for 48 h, cells were treated with Nec-1 (30  $\mu$ M), z-VAD-fmk (20  $\mu$ M), NSA (10  $\mu$ M), Mdivi-1 (20  $\mu$ M) or olaparib (30  $\mu$ M) for 1 h. Cell viability were determined by MTS assay. (B, C) Cells were treated with Nec-1 before the addition of oxaliplatin for the indicated hours, the activity of LDH and release of CypA with HMGB1 were detected as mentioned above. (D, E) Cells were transfected with NC (negative control), three individual RIP1 (001–003) or RIP3 (004–006) siRNAs for 72 h, the RNAi efficiency were determined by Western blotting. (F) After transfection with the indicated siRNAs for 48 h, cells were stimulated with oxaliplatin for a further 48 h and cell viability was determined by MTS assay.

Induction of necroptosis by death ligand has recently been shown to involve sequential activation of MLKL, PGAM5 and Drp1 downstream of RIP1 and RIP3. Nec-1 significantly protected SGC-7901 cells from dying, whereas NSA could barely attenuate cell death. Mdivi-1 displayed extensive toxicity towards SGC-7901 cells, even though it had partial inhibitory effect. Recent reports showed that necrosis induced by shikonin [17], cadmium [18] and glutamate [19] can also be inhibited by Nec-1. But Nec-1 is apparently not a ubiquitous inhibitor for all kinds of necrotic cell death. This characteristic is similar to that of z-VAD-fmk, which cannot block all types of apoptosis. In most cases, Nec-1 is becoming an important tool for evaluating the contribution of necrotic cell death in experimental disease models. Besides, siRNA knockdown of RIP1

but not RIP3 could partially suppress cell death. It was reported that siRNA-mediated silencing of RIP1 could inhibit z-VAD-fmk-induced necrosis, but not TNF- $\alpha$ -induced necrosis [20]. Besides RIP1, Nec-1 also targets other factors crucial for necrosis induction. These results demonstrated that RIP1 is a key molecule in oxaliplatin-induced cell death, but RIP3 and its downstream components are not involved in the death program.

DNA-damage-induced necrosis involves a large network of molecular determinants: DNA-damage repair proteins (PARP-1 and H2AX), kinases (RIP1, ataxia telangiectasia mutated [ATM] and DNA dependent protein kinase [DNA-PK]), proteases (calpains), Bcl-2 family members (Bid and Bax), mitochondrial effectors (AIF), and Dnases (CypA) [21]. Oxaliplatin-induced DNA damage caused the

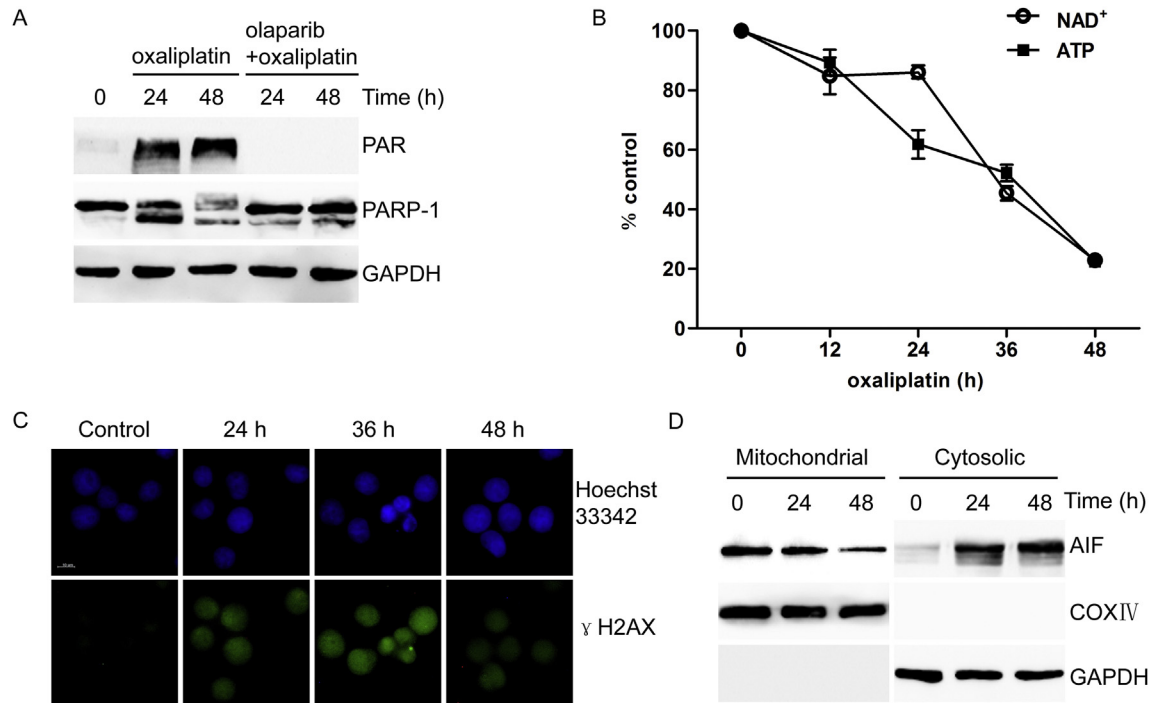


**Fig. 4.** Oxaliplatin induces H2AX phosphorylation and AIF translocation. (A) Western blotting of PAR and PARP-1 from cells treated with oxaliplatin in the presence or absence of olaparib. (B) Quantification of intracellular NAD<sup>+</sup> and ATP levels in cells treated with oxaliplatin at the indicated time. (C) Immunofluorescent staining of γH2AX detected in cells left untreated (Control) or treated with oxaliplatin and stained with Hoechst 33342 (to visualize nuclei) or a specific γH2AX antibody. Representative cells are shown. Bar: 10 μm. (D) Mitochondrial and cytosolic fractions recovered from cells after oxaliplatin treatment were probed for AIF detection. GAPDH (cytosolic marker) and COX IV (mitochondrial marker) were used to control protein loading and fractionation quality.

disproportionate activation of PARP-1, phosphorylation of H2AX and AIF translocation. Inhibition of the PARP-1 pathway by olaparib could protect against oxaliplatin-induced cell death, thus confirming that PARP-1 activation is mainly responsible for the cytotoxicity of oxaliplatin. Most cancer cells using aerobic glycolysis to support their bioenergetics undergo rapid energy depletion caused by PARP-1 overactivation [22]. It should be noted that this study has concentrated on the role of PARP-1, H2AX and AIF, the detailed signaling pathway remains to be clarified.

In summary, we demonstrated that oxaliplatin triggered necrosis as well as apoptosis in gastric cancer SGC-7901 cells. Although caspase cascades were activated, it appeared dispensable for killing. Necrosis may even occur without caspase activity being inhibited. In fact, apoptosis and necrosis are not mutually exclusive processes, they may function as reciprocal backup mechanisms of cellular demise. In essence, necrosis has probably been targeted unwittingly since the beginning of chemotherapy. Regardless, the ability to bypass canonical apoptotic pathway to kill cancer cells may be of therapeutic advantage, especially to kill those apoptosis-resistant cancer cells.

#### Conflict of interest

None.

#### Acknowledgments

This work was supported by grants from National Natural Science Foundation of China (No. 81071809) and Natural Science Research Project of Anhui Higher Education Institutions, China (No. KJ2014A113).

#### Transparency document

Transparency document related to this article can be found online at <http://dx.doi.org/10.1016/j.bbrc.2015.03.003>.

#### References

- [1] N. Vanlangenakker, T. Vanden Berghe, P. Vandenabeele, Many stimuli pull the necrotic trigger, an overview, *Cell. Death. Differ.* 19 (2012) 75–86.
- [2] S. He, L. Wang, L. Miao, T. Wang, F. Du, L. Zhao, X. Wang, Receptor interacting protein kinase-3 determines cellular necrotic response to TNF- $\alpha$ , *Cell* 137 (2009) 1100–1111.
- [3] A. Degterev, J. Hitomi, M. Gerscheid, I.L. Ch'en, O. Korkina, X. Teng, D. Abbott, G.D. Cuny, C. Yuan, G. Wagner, S.M. Hedrick, S.A. Gerber, A. Lugovskoy, J. Yuan, Identification of RIP1 kinase as a specific cellular target of necrostatins, *Nat. Chem. Biol.* 4 (2008) 313–321.
- [4] L. Sun, H. Wang, Z. Wang, S. He, S. Chen, D. Liao, L. Wang, J. Yan, W. Liu, X. Lei, X. Wang, Mixed lineage kinase domain-like protein mediates necrosis signaling downstream of RIP3 kinase, *Cell* 148 (2012) 213–227.
- [5] Z. Wang, H. Jiang, S. Chen, F. Du, X. Wang, The mitochondrial phosphatase PGAM5 functions at the convergence point of multiple necrotic death pathways, *Cell* 148 (2012) 228–243.
- [6] C.C. Alano, W. Ying, R.A. Swanson, Poly(ADP-ribose)polymerase-1-mediated cell death in astrocytes requires NAD<sup>+</sup> depletion and mitochondrial permeability transition, *J. Biol. Chem.* 279 (2004) 18895–18902.
- [7] R.S. Moubarak, V.J. Yuste, C. Artus, A. Bouharrou, P.A. Greer, J. Menissier-de Murcia, S.A. Susin, Sequential activation of poly(ADP-ribose)polymerase 1, calpains, and BAX is essential in apoptosis-inducing factor-mediated programmed necrosis, *Mol. Cell. Biol.* 27 (2007) 4844–4862.
- [8] L. Cabon, P. Galán-Malo, A. Bouharrou, L. Delavallée, M.N. Brunelle-Navas, H.K. Lorenzo, A. Gross, S.A. Susin, BID regulates AIF-mediated caspase-independent necroptosis by promoting BAX activation, *Cell. Death. Differ.* 19 (2012) 245–256.
- [9] C. Artus, H. Boujrad, A. Bouharrou, M.N. Brunelle, S. Hoos, V.J. Yuste, P. Lenormand, J.C. Rousselle, A. Namane, P. England, H.K. Lorenzo, S.A. Susin, AIF promotes chromatinolysis and caspase-independent programmed necrosis by interacting with histone H2AX, *EMBO. J.* 29 (2010) 1585–1599.
- [10] A. Degterev, Z. Huang, M. Boyce, Y. Li, P. Jagtap, N. Mizushima, G.D. Cuny, T.J. Mitchison, M.A. Moskowitz, J. Yuan, Chemical inhibitor of nonapoptotic cell death with therapeutic potential for ischemic brain injury, *Nat. Chem. Biol.* 1 (2005) 112–119.

- [11] J.B. Engel, T. Martens, J.C. Hahne, S.F. Häusler, M. Krockenberger, S. Segerer, A. Djakovic, S. Meyer, J. Dietl, J. Wischhusen, A. Honig, Effects of Iobaplatin as a single agent and in combination with TRAIL on the growth of triple-negative p53-mutated breast cancers in vitro, *Anticancer. Drugs* 23 (2012) 426–436.
- [12] H. Sawai, N. Domae, Discrimination between primary necrosis and apoptosis by necrostatin-1 in annexin V-positive/propidium iodide-negative cells, *Biochem. Biophys. Res. Commun.* 411 (2011) 569–573.
- [13] D.E. Christofferson, J. Yuan, Cyclophilin A release as a biomarker of necrotic cell death, *Cell. Death. Differ.* 17 (2010) 1942–1943.
- [14] R. Shindo, H. Kakehashi, K. Okumura, Y. Kumagai, H. Nakano, Critical contribution of oxidative stress to TNF $\alpha$ -induced necroptosis downstream of RIPK1 activation, *Biochem. Biophys. Res. Commun.* 436 (2013) 212–216.
- [15] S.C. Lim, J.E. Choi, H.S. Kang, S.I. Han, Ursodeoxycholic acid switches oxaliplatin-induced necrosis to apoptosis by inhibiting reactive oxygen species production and activating p53-caspase8 pathway in HepG2 hepatocellular carcinoma, *Int. J. Cancer* 126 (2010) 1582–1595.
- [16] J. Hitomi, D.E. Christofferson, A. Ng, J. Yao, A. Degterev, R.J. Xavier, J. Yuan, Identification of a molecular signaling network that regulates a cellular necrotic cell death pathway, *Cell* 135 (2008) 1311–1323.
- [17] W. Han, L. Li, S. Qiu, Q. Lu, Q. Pan, Y. Gu, J. Luo, X. Hu, Shikonin circumvents cancer drug resistance by induction of a necroptotic death, *Mol. Cancer. Ther.* 6 (2007) 1641–1649.
- [18] T.S. Hsu, P.M. Yang, J.S. Tsai, L.Y. Lin, Attenuation of cadmium-induced necrotic cell death by necrostatin-1: potential necrostatin-1 acting sites, *Toxicol. Appl. Pharmacol.* 235 (2009) 153–162.
- [19] X. Xu, C.C. Chua, J. Kong, R.M. Kostrzewa, U. Kumaraguru, R.C. Hamdy, B.H. Chua, Necrostatin-1 protects against glutamate-induced glutathione depletion and caspase-independent cell death in HT-22 cells, *J. Neurochem.* 103 (2007) 2004–2014.
- [20] Y. Cho, T. McQuade, H. Zhang, J. Zhang, F.K. Chan, RIP1-dependent and independent effects of necrostatin-1 in necrosis and T cell activation, *PLoS One* 6 (2011) e23209.
- [21] M. Baritaud, L. Cabon, L. Delavallée, P. Galán-Malo, M.E. Gilles, M.N. Brunelle-Navas, S.A. Susin, AIF-mediated caspase-independent necroptosis requires ATM and DNA-PK-induced histone H2AX Ser139 phosphorylation, *Cell. Death. Dis.* 3 (2012) e390.
- [22] W.X. Zong, D. Ditsworth, D.E. Bauer, Z.Q. Wang, C.B. Thompson, Alkylating DNA damage stimulates a regulated form of necrotic cell death, *Genes. Dev.* 18 (2004) 1272–1282.